apertures," *IEEE Trans. Antennas Propagat.*, vol. AP-25, pp. 198–205, Mar. 1977.

[3] R. W. Latham, "Small holes in cable shields," Interaction Notes, Note 118, Sept. 1972.

[4] K. S. H. Lee, Ed., "EMP interaction: Principles, techniques, and reference data," Air Force Weapons Lab. Tech. Rep. AFWL-TR-80-402, pp. 514, 515, Dec. 1979.

[5] K. F. Casey, "Static electric and magnetic field penetration of a spherical shield through a circular aperture," Interaction Notes, Note 381, Feb. 1980.

[6] K. C. Lang, "Babinet's principle for a perfectly conducting screen with aperture covered by a resistive sheet," *IEEE Trans. Antennas Propagat.*, vol. AP-21, pp. 738–740, Sept. 1973.

[7] R. F. Harrington and J. R. Mautz, "Comments on 'Babinet's principle for a perfectly conducting screen with aperture covered by a resistive sheet," *IEEE Trans. Antennas Propagat.*, vol. AP-22, p. 842, Nov. 1974.

[8] C. E. Baum and B. K. Singaraju, "Generalization of Babinet's principle in terms of the combined fields to include impedance

[9] T. B. A. Senior, "Some extensions of Babinet's principle," *J. Acoust. Soc. Amer.*, vol. 58, pp. 501–503, Aug. 1975.

[10] R. W. Latham and K. S. H. Lee, "Magnetic field leakage into a semi-infinite pipe," *Can. J. Phys.*, vol. 46, pp. 1455–1462, 1968.

[11] J. P. Quine and H. Q. Totten, "Radar modulator suppression—Cabinet aperture leakage," in *Proc. Conf. on Radio Interference Reduction* (1954), pp. 220–232.

[12] J. P. Quine, "Theoretical formulas for calculating the shielding effectiveness of perforated sheets and wire mesh screens," in *Proc. Conf. on Radio Interference Reduction* (1957), pp. 315–329.

[13] K. F. Casey, "Electromagnetic shielding by advanced composite materials," Interaction Notes, Note 341, 1977.

[14] I. N. Sneddon, *Mixed Boundary Value Problems in Potential Theory.* Amsterdam, The Netherlands: North-Holland, 1966, pp. 106 ff.

[15] A. M. J. Davis, "Waves in the presence of an infinite dock with gap," *J. Inst. Math. Appl.*, vol. 6, pp. 141–156, 1970.

Absorbing Boundary Conditions for the Finite-Difference Approximation of the Time-Domain Electromagnetic-Field Equations

GERRIT MUR

Abstract—When time-domain electromagnetic-field equations are solved using finite-difference techniques in unbounded space, there must be a method limiting the domain in which the field is computed. This is achieved by truncating the mesh and using absorbing boundary conditions at its artificial boundaries to simulate the unbounded surroundings. This paper presents highly absorbing boundary conditions for electromagnetic-field equations that can be used for both two- and three-dimensional configurations. Numerical results are given that clearly exhibit the accuracy and limits of applicability of highly absorbing boundary conditions. A simplified, but equally accurate, absorbing condition is derived for two-dimensional time-domain electromagnetic-field problems.

Key Words—Electromagnetic-field equations, time domain, finite-difference approximation, absorbing boundary conditions.

I. INTRODUCTION

THE THREE-DIMENSIONAL finite-difference formulation [1] of time-domain electromagnetic-field problems is a convenient tool for solving scattering problems. The main advantages of such a method are that it can be easily applied to (infinitely) conducting obstacles and/or to dielectric and

magnetic obstacles which can be either homogeneous or inhomogeneous. The obstacles can be of arbitrary shape. Furthermore, finite-difference techniques provide a very efficient way of solving Maxwell's equations [2]. In a finite-difference method, a space-time mesh is introduced and Maxwell's equations are replaced by a system of finite-difference equations on the mesh. The difficulty encountered when trying to solve field problems in this way arises from the fact that scattering problems are usually *open* problems, i.e., the domain in which the field has to be computed is unbounded. Since no computer can store an unlimited amount of data, a method has to be used for limiting the domain in which the field is computed. This is done by using a mesh of limited size, but one large enough to fully contain the obstacle, and by using a boundary condition on the outer surface of the mesh such that the unbounded surrounding is modeled as accurately as possible. Boundary conditions of this type are called absorbing boundary conditions. For finite-difference approximations of Maxwell's equations, absorbing boundary conditions have been described by Taylor et al. [3], who use a simple extrapolation method, and by Taflove and Brodwin [4], who simulate the outgoing waves and use an averaging process in an attempt to account for all possible angles of propagation of the outgoing waves. An alternative method, suggested by Taflove [5], is to introduce losses in the region that surrounds the structure to be modeled, thus absorbing both the outgoing waves and

the waves that are reflected by the boundaries of the mesh. Numerical experiments, however, have shown that, in order to obtain accurate results, a relatively thick conducting layer is required which makes this way of absorbing the outgoing waves inefficient. Merewether [6] and Kunz and Lee [7] use the radiation condition at large distances from the center of the scatterer to obtain an absorbing boundary condition.

The absorbing boundary conditions mentioned above, although useful as first approximations, have the disadvantage of causing considerable reflections when the fields near the boundary of the mesh do not propagate in a specific direction (either the direction normal to the boundary of the mesh or the radial direction from the center of the obstacle). Furthermore, no general theory for improving upon these approximations is available. In this paper, a potentially superior method to those given above is derived for both the two- and three-dimensional electromagnetic-field equations; it is similar to the scalar derivation of Engquist and Majda [8]. The first approximation in the sense of this method appears to be comparable to those given above. The second and higher approximations are less subject to reflection problems, especially for fields grazing the outer boundary, making them highly absorbing boundary conditions. For two-dimensional fields, a simplified, but equally accurate, absorbing boundary condition will be derived. Numerical results will be presented to elucidate the usefulness of highly absorbing boundary conditions.

II. FINITE-DIFFERENCE APPROXIMATION OF MAXWELL'S EQUATIONS

Since, in this paper, we do not concern ourselves with obstacles or inhomogeneities but with the homogeneous region that surrounds them, we can, without loss of generality, confine our attention to Maxwell's equations for a vacuum region. In rectangular Cartesian coordinates we have

$$\mu_0 \partial_t H = - \nabla \times E \tag{1a}$$

$$\epsilon_0 \partial_t E = \nabla \times H \tag{1b}$$

where ϵ_0 and μ_0 denote the permittivity and the permeability of a vacuum, respectively. We now introduce a finite-difference approximation of (1) and, following Yee's notation [1], we denote a mesh point as

$$(i, j, k) = (i\delta, j\delta, k\delta)$$

where $\delta = \delta x = \delta y = \delta z$ is the space increment, and any function of space and time as

$$F^n(i, j, k) = F(i\delta, j\delta, k\delta, n\delta t)$$

where δt is the time increment. By positioning the field components of E and H on the mesh in the way that is depicted in Fig. 1 and evaluating E and H at alternate half-time steps, Yee obtained finite-difference expressions that have a local trucation error of the second order in all increments. The finite-difference approximation for the x-component of (1a) and
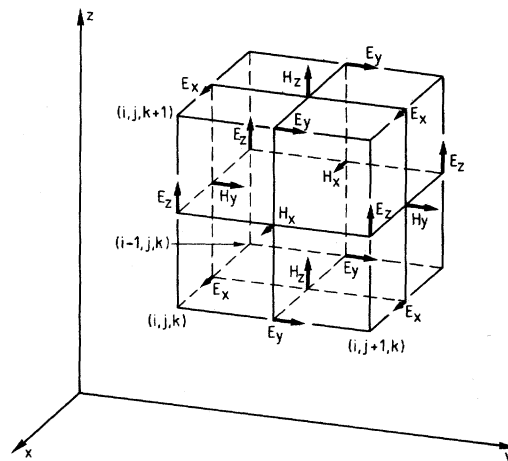

Fig. 1.   The positions of the field components in Yee's mesh.

(1b) now reads

$$H_x^{n+1/2}(i, j + 1/2, k + 1/2)$$

$$= H_x^{n-1/2}(i, j + 1/2, k + 1/2) - (\delta t / \mu_0 \delta)$$

$$\cdot (E_z^n(i, j + 1, k + 1/2) - E_z^n(i, j, k + 1/2)$$

$$- E_y^n(i, j + 1/2, k + 1) + E_y^n(i, j + 1/2, k)) \tag{2a}$$

$$E_x^{n+1}(i + 1/2, j, k)$$

$$= E_x^n(i + 1/2, j, k) + (\delta t / \epsilon_0 \delta)$$

$$\cdot (H_z^{n+1/2}(i + 1/2, j + 1/2, k)$$

$$- H_z^{n+1/2}(i + 1/2, j - 1/2, k)$$

$$- H_y^{n+1/2}(i + 1/2, j, k + 1/2)$$

$$+ H_y^{n+1/2}(i + 1/2, j, k - 1/2)). \tag{2b}$$

Similar finite-difference approximations for the y- and z-components of (1) can easily be derived. The condition for stability of (2) is

$$\delta t \leqslant \delta / (c_0 \sqrt{3}) \tag{3}$$

where $c_0 = (\epsilon_0 \mu_0)^{-1/2}$ denotes the speed of light in vacuo.

For a two-dimensional problem, we use only a single plane in the mesh and consequently (2) is considerably simplified. The condition for stability then reads

$$\delta t \leqslant \delta / (c_0 \sqrt{2}). \tag{4}$$

In each of the coordinate directions, the mesh is truncated by enclosing it between two planes that are normal to the relevant coordinate axis and pass through mesh points (i, j, k), i, j, k integer. We then observe from Fig. 1 that all components of the electric-field vector E occurring in (2) applied to a particular point in the boundary of the mesh are tangential to this boundary while the relevant components of the magnetic-field vector H are normal to it. The latter field components can be evaluated by using the relevant finite-dif-

ference equation. The E-field components, however, cannot be evaluated in this way since this would require H-field components that are outside the mesh. In the next section, we shall describe absorbing boundary conditions that can be used for computing these E-field components. For absorbing boundary conditions, it is assumed that the fields near the boundary are outgoing waves and, therefore, they can be applied to only scattered fields, i.e., those that find their origin somewhere near the center of the mesh. Consequently, incident fields, if present on the mesh, should be subtracted from the total field near the boundary of the mesh. Finally, we note that, upon elimination of H from (2), we obtain

$$(\partial_x^2 + \partial_y^2 + \partial_z^2 - c_0^{-2}\partial_t^2)E = 0 \qquad (5)$$

i.e., each component of the electric field independently satisfies the three-dimensional wave equation.

III. ABSORBING BOUNDARY CONDITIONS

In the previous section, we saw that absorbing boundary conditions for Maxwell's equations on the mesh depicted in Fig. 1 require absorbing boundary conditions for the three components of the electric field only. We also saw that each of these field components satisfies the three-dimensional scalar wave equation

$$(\partial_x^2 + \partial_y^2 + \partial_z^2 - c_0^{-2}\partial_t^2)W = 0. \qquad (6)$$

In this section, we will present the necessary boundary conditions by using the method that is described in detail by Engquist and Majda [8]. We shall assume, without loss of generality, that the mesh is located in the region $0 \leqslant x$, and give boundary conditions for the plane $x = 0$.

A space-time plane-wave constituent traveling in the direction of decreasing x, with inverse velocity components s_x, s_y and s_z such that $s_x^2 + s_y^2 + s_z^2 = c_0^{-2}$, can be written as

$$W = \text{Re } (\psi(t + (c_0^{-2} - s_y^2 - s_z^2)^{1/2} x$$
$$+ s_y y + s_z z)) \qquad (7)$$

with $\text{Re}(c_0^{-2} - s_y^2 - s_z^2)^{1/2} \geqslant 0$. For this outgoing wave, the first-order boundary condition

$$(\partial_x - c_0^{-1}(1 - (c_0 s_y)^2 - (c_0 s_z)^2)^{1/2}\partial_t)W|_{x=0} = 0 \qquad (8)$$

would, for fixed values of s_y and s_z, determine a W on the outer surface that is consistent with an outgoing wave, i.e., it is absorbed. Since we do not know the angle of incidence of the wave approaching $x = 0$, an approximation in (8) is made. Writing

$$(1 - (c_0 s_y)^2 - (c_0 s_z)^2)^{1/2}$$
$$= 1 + O((c_0 s_y)^2 + (c_0 s_z)^2) \qquad (9)$$

we obtain as a first approximation

$$(\partial_x - c_0^{-1}\partial_t)W|_{x=0} = 0. \qquad (10)$$

Use of the next approximation to the square root

$$(1 - (c_0 s_y)^2 - (c_0 s_z)^2)^{1/2}$$
$$= 1 - \tfrac{1}{2}((c_0 s_y)^2 + (c_0 s_z)^2)$$
$$+ O(((c_0 s_y)^2 + (c_0 s_z)^2)^2) \qquad (11)$$

yields the second approximation of the boundary condition

$$(c_0^{-1}\partial_{xt}^2 - c_0^{-2}\partial_t^2 + \tfrac{1}{2}(\partial_y^2 + \partial_z^2))W|_{x=0} = 0. \qquad (12)$$

From (10) and (12), approximations of W can be determined on the outer boundary. Engquist and Majda, who arrived at the same boundary conditions using a different method, prove that these boundary conditions give well-posed initial-boundary-value problems. They also give a third approximation that they claim to be stable. Numerical experiments, in a two-dimensional configuration, with a difference approximation of the latter boundary condition, however, showed instabilities for values of $c_0 \delta t/\delta$ near the maximum that is given by (4).

For two-dimensional electromagnetic-field problems, it is possible to simplify the second approximation. Assuming that the fields do not depend on z and are E-polarized, i.e., $E = E_z i_z$ and $H = H_x i_x + H_y i_y$, (12) applies to E_z only. Now, in this case, we have from (1a)

$$\mu_0 \partial_t H_x = -\partial_y E_z. \qquad (13)$$

Substituting (13) in (11), ($\partial_z \equiv 0$), with $W = E_z$, integrating with respect to t and using $E_z = 0$ for $t < 0$, we obtain

$$(\partial_x E_z - c_0^{-1}\partial_t E_z - (c_0 \mu_0/2)\partial_y H_x)_{x=0} = 0 \qquad (14)$$

which boundary condition is much simpler than (12) but still of the same order of approximation. We observe that the first two terms of (14) reduce to the first approximation. A similar boundary condition for the case of H-polarization can easily be derived.

IV. FINITE-DIFFERENCE APPROXIMATIONS OF ABSORBING BOUNDARY CONDITIONS

In this section, we present the finite-difference approximation of the absorbing boundary conditions from Section III. These approximations have a local truncation error of the second order in all increments. As we have seen above, we need absorbing boundary conditions for the E-field components that are tangential to the boundary of interest. Therefore, boundary conditions for the plane $x = 0$ are expressed in terms of E_y and E_z. We shall give the discretized form of the boundary condition for E_z at this boundary, the boundary conditions for E_y and the boundary conditions on the other planes following easily from the one for E_z. The finite-difference approximation of (10) was derived using centered differences in both the space and the time increments, it has a local truncation error of the second order in all increments. We prefer to present the actual formulas in a form that is directly manageable for the computer program. The first approxima-

tion (10) for E_z is discretized as follows:

$$E_z^{n+1}(0,j,k+1/2 = E_z^n(1,j,k+1/2)$$

$$+\frac{c_0\delta t - \delta}{c_0\delta t + \delta}(E_z^{n+1}(1,j,k+1/2)$$

$$-E_z^n(0,j,k+1/2)). \qquad (15)$$

The second approximation (12) for E_z at the boundary $x = 0$ is discretized as

$$E_z^{n+1}(0,j,k+1/2)$$

$$=-E_z^{n-1}(1,j,k+1/2)+\frac{c_0\delta t-\delta}{c_0\delta t+\delta}(E_z^{n+1}(1,j,k+1/2)$$

$$+E_z^{n-1}(0,j,k+1/2))+\frac{2\delta}{c_0\delta t+\delta}(E_z^n(0,j,k+1/2)$$

$$+E_z^n(1,j,k+1/2))+\frac{(c_0\delta t)^2}{2\delta(c_0\delta t+\delta)}$$

$$\cdot(E_z^n(0,j+1,k+1/2)-2E_z^n(0,j,k+1/2)$$

$$+E_z^n(0,j-1,k+1/2)+E_z^n(1,j+1,k+1/2)$$

$$-2E_z^n(1,j,k+1/2)+E_z^n(1,j-1,k+1/2)$$

$$+E_z^n(0,j,k+3/2)-2E_z^n(0,j,k+1/2)$$

$$+E_z^n(0,j,k-1/2)+E_z^n(1,j,k+3/2)$$

$$-2E_z^n(1,j,k+1/2)+E_z^n(1,j,k-1/2)). \qquad (16)$$

Finally, the second approximation (14) for the two-dimensional problem is discretized as

$$E_z^{n+1}(0,j)=E_z^n(1,j)+\frac{c_0\delta t-\delta}{c_0\delta t+\delta}(E_z^{n+1}(1,j)$$

$$-E_z^n(0,j))-\frac{\mu_0 c_0}{2(c_0\delta t+\delta)}$$

$$(H_x^{n+1/2}(0,j+1/2)-H_x^{n+1/2}(0,j-1/2)$$

$$+H_x^{n+1/2}(1,j+1/2)-H_x^{n+1/2}(1,j-1/2)) \qquad (17)$$

where we have deleted the z-dependence of the fields from our notation since the value of z is the same in all terms. Centered differences were used for deriving (16) and (17) and these finite-difference approximations also have a local truncation error of the second order in all increments. We note that the discretization of the first approximation (15) is identical to the discretization in [8]. The discretization of the second approximation (16), however, differs from the one in [8]. Ours has the advantage that it can be used closer to the vertices of the mesh that it requires less storage.

V. NUMERICAL RESULTS

In this section, we present numerical results that show the efficiency of highly absorbing boundary conditions. Since we need a relatively large-size mesh to exhibit clearly the proper-
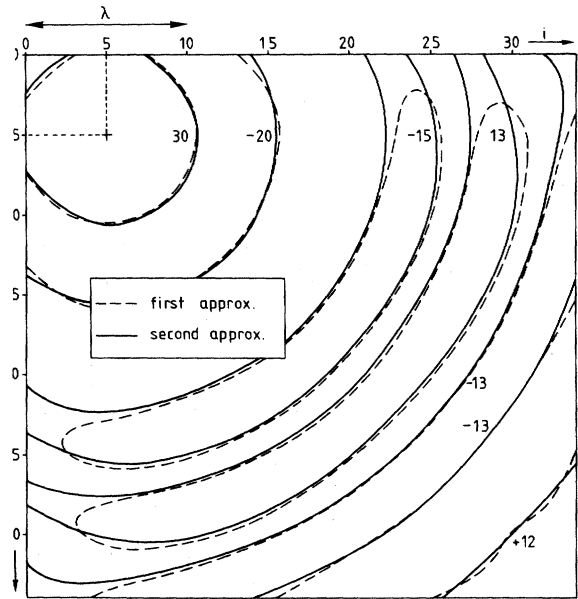

Fig. 2. Contour plot of the radiation pattern, after 141 time steps, of an isotropic source located at node (5, 5) of a 35*35-node mesh (arbitrary units).

ties of absorbing boundary conditions, we shall present results for two-dimensional configurations only; three-dimensional meshes of considerable size would give rise to storage requirements that were too large for the computer that was available to the author at the time this research was carried out. The insight gained by studying a two-dimensional configuration can easily be applied to three-dimensional configurations since the structure of (16) is the same for two- and three-dimensional problems. (The two-dimensional form of (16) is obtained by deleting from it the differentiations along the axis of cylindricity.) We present results for fields that do not depend on z and are E-polarized (i.e., $E = E_z i_z$). A square two-dimensional mesh is used ($0 \leq i \leq 34, 0 \leq j \leq 34$) with absorbing boundary conditions on all four sides. We have a monochromatic isotropic point source of wavelength λ that is switched on at $t = 0$ and we use $\delta = \delta_x = \delta_y = 2c_0\delta t = 0.1\lambda$. This point source is modeled by adding a term representing a current

$$I_z(t) = C \sin (2\pi c_0 t/\lambda)\epsilon(t) \qquad (18)$$

at $r_s = (x_s, y_s) = (i\delta, j\delta)$ to the relevant finite-difference equation. In (18), $\epsilon(t)$ denotes the Heaviside unit-step function. The results are given after 141 steps.

An isotropic point source has a circular radiation pattern and we investigate how well this pattern is maintained on the truncated mesh. Fig. 2 gives a contour plot of the radiation pattern on the mesh for a point source that is located at node $(i, j) = (5, 5)$, which location was chosen to show, as clearly as possible, the efficiency of highly absorbing boundary conditions. The numbers in the contour plot are proportional to the local electric-field strength.

The contour plot is given for both the first and the second approximation. The first approximation turns out to yield relatively poor results, especially at large distances from the source. With the second approximation, however, an almost circular pattern is obtained with only slight deformations at
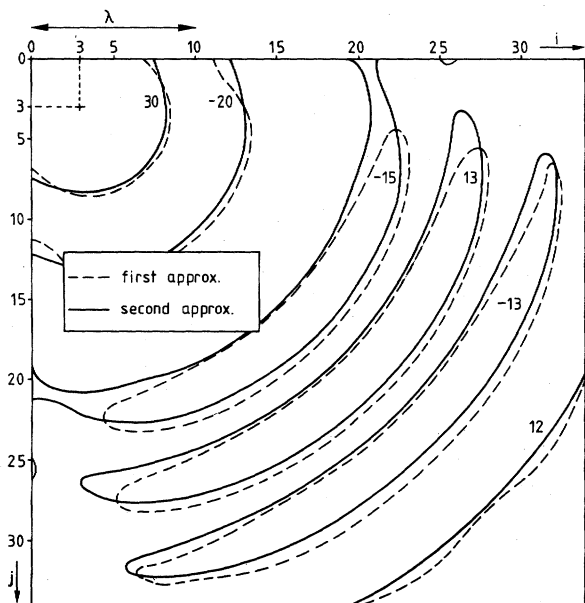
Fig. 3. Contour plot of the radiation pattern, after 141 time steps, of an isotropic source located at node (3, 3) of a 35*35-node mesh (arbitrary units).
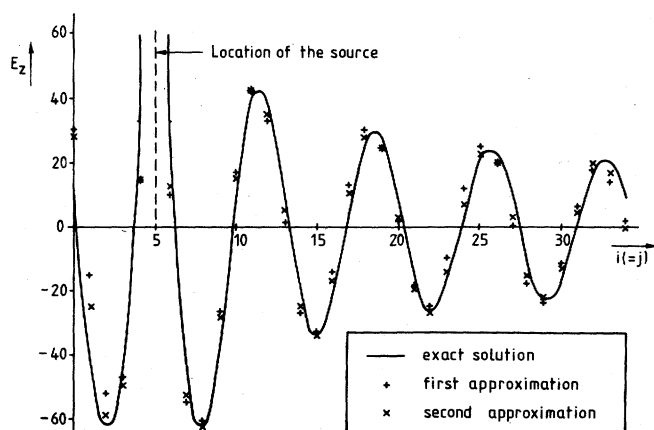

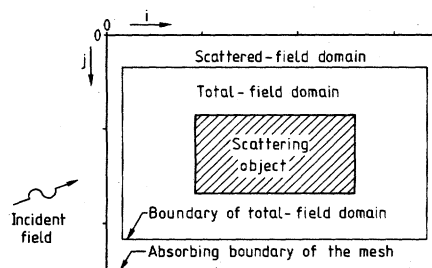Fig. 4. A comparison of the results on the diagonal of the mesh of Fig. 2 with the exact solution.

Fig. 5. The domain occupied by the mesh with the obstacle, the domain where the total field is computed, and the domain where the scattered field is computed (two-dimensional configuration).

points near the boundaries and far away from the source. These errors are caused by the fact that waves with grazing incidence on a boundary are not well absorbed, but partly reflected. For comparison, Fig. 3 gives the contour plot of the field of the same source that is now located closer to the boundary of the mesh, at node $(i, j) = (3, 3)$. A comparison with Fig. 2 is possible since the same contour lines are given. From Fig. 3, we observe that, near the boundary of the mesh, the second approximation is not accurate enough for sources this close to the boundary. It can be concluded that, on a mesh of the given dimensions, accurate results are obtained when the second approximation is used and when the source of the scattered field is located at about five or more nodes from the boundary of the mesh. With the first approximation, less accurate results are obtained and the source of the scattered field should be relatively far away from the boundary. Since (16) is easy to implement, it is advantageous to use the second approximation.

As to the simplified second approximation for two-dimensional fields (17), we note that it gives exactly the same results as the more complicated one that follows from (16).

For the point source under consideration, the exact radiated field is the solution of

$$(\partial_x^2 + \partial_y^2 - c_0^{-2}\partial_t^2)E_z = \mu_0 \partial_t I_z(t)\delta(r - r_s) \qquad (19)$$

that is rotationally symmetric around r_s and that consists of outgoing waves. This solution is easily obtained [10] as

$$E_z(r, t) = -(\mu_0/2\pi) \int_0^\infty \partial_t I_z(t - (|r - r_s|^2 + \zeta^2)^{1/2}/c_0)$$

$$\cdot (|r - r_s|^2 + \zeta^2)^{-1/2} d\zeta. \qquad (20)$$

In Fig. 4, this exact solution is plotted as a function of the distance from the point source and at the same instant in time as the results that are given in Fig. 2. For comparison we have,

in Fig. 4, also given the finite-difference results that are obtained on the diagonal of the mesh of Fig. 2 that passes through the point source. It turns out that, considering the fact that we have a relatively coarse mesh ($\delta = \lambda/10$), we have obtained accurate results.

VI. THE INCIDENT FIELD

In the present paper, we have used a point source to generate outgoing waves at the boundaries of the mesh. In practice, the outgoing waves are not generated by a source in the mesh but represent the scattered field E^s that is caused by the presence of an obstacle that scatters the incident field E^i (the incident field is assumed to be known.) If maximum accuracy is desired, it is advantageous to compute the total field $E = E^s + E^i$ rather than the scattered field [5], [9], especially in those regions where the scattered field almost cancels the incident field (behind or in the interior of scattering objects). Absorbing boundary conditions, however, cannot be applied to the total field.

To overcome this difficulty, a boundary can be introduced that is located close to the absorbing boundaries of the mesh (see Fig. 5.) Inside this boundary the total field is computed, outside it the scattered field is computed, thus allowing the application of absorbing boundary conditions. When (2) is evaluated for the total (scattered) field at a node inside (outside) this boundary, but adjacent to it, the total field will often be required from nodes that are located outside (inside) it. For the relevant nodes, (2) is modified. When computing the total field inside the boundary, the incident field is added to the scattered field that is obtained from nodes outside the

boundary and, similarly, when computing the scattered field outside the boundary, the incident field is subtracted from the total field obtained from inside the boundary. Since the incident field is known exactly at any place or instant in time the above procedure does not involve any approximations, moreover, it does not require any storage nor does it cause any spurious wave reflection.

ACKNOWLEDGMENT

The author wants to thank A. T. de Hoop for his suggestions concerning the work presented in this paper.

REFERENCES

[1] K. S. Yee, "Numerical solution of initial boundary value problems involving Maxwell's equations in isotropic media," *IEEE Trans. Antennas Propagat.*, vol. AP-14, pp. 302–307, May 1966.

[2] C. L. Longmire, "State of the art in IEMP and SGEMP calculations," *IEEE Trans. Nucl. Sci.*, vol. NS-22, pp. 2340–2344, Dec. 1975.

[3] C. D. Taylor, D.-H. Lam, and T. H. Shumpert, "Electromagnetic pulse scattering in time-varying inhomogeneous media," *IEEE Trans. Antennas Propagat.*, vol. AP-17, pp. 585–589, Sept. 1969.

[4] A. Taflove and M. E. Brodwin, "Numerical solution of steady-state electromagnetic scattering problems using the time dependent Maxwell's equations," *IEEE Trans. Microwave Theory Tech.*, vol. MTT-23, pp. 623–630, Aug. 1975.

[5] A. Taflove, "Application of the finite-difference time-domain method to sinusoidal steady-state electromagnetic penetration problems," *IEEE Trans. Electromagn. Compat.*, vol. EMC-22, pp. 191–202, 1980.

[6] D. E. Merewether, "Transient currents induced on a metallic body of revolution by an electromagnetic pulse," *IEEE Trans. Electromagn. Compat.*, vol. EMC-13, pp. 41–44, May 1971.

[7] K. S. Kunz and K.-M. Lee, "A three-dimensional finite-difference solution of the external response of an aircraft to a complex transient EM environment: Part I—The method and its implementation," *IEEE Trans. Electromagn. Compat.*, vol. EMC-20, pp. 328–333, May 1978.

[8] B. Engquist and A. Majda, "Absorbing boundary conditions for the numerical simulation of waves," *Math. Comp.*, vol. 31, pp. 629–651, July 1977.

[9] R. Holland, L. Simpson, and K. S. Kunz, "Finite-difference analysis of EMP coupling to lossy dielectric structures," *IEEE Trans. Electromagn. Compat.*, vol. EMC-22, pp. 203–209, 1980.

[10] J. D. Achenbach, *Wave Propagation in Elastic Solids*. Amsterdam, The Netherlands: North-Holland, 1973, ch. 3, p. 94.

Numerical Determination of Induced Currents in Humans and Baboons Exposed to 60-Hz Electric Fields

RONALD J. SPIEGEL, MEMBER, IEEE

Abstract—In order to extrapolate 60-Hz electric-field effects on experimental animals (baboons) in terms of equivalent effects on man, scaling relations for the induced current densities have been developed by utilizing advanced computer-modeling techniques. Humans and baboons were modeled by a large number of small cubical blocks that were arranged to obtain the best possible fit to the contour of the object. Internal current densities for the models were calculated by the solution of an integral equation for the induced polarization at the center of each block.

Key Words—Radiation hazards, humans and baboons, induced currents, 60-Hz fields, computer modeling.

INTRODUCTION

THE ELECTRIC POWER industry is currently developing and studying electric transmission lines with operating voltages exceeding 765 kV [1]. While the increased efficiency of ultra-high-voltage lines makes them highly desirable, a pos-

sible serious question arises as to what effects the high-strength electric fields will have on living organisms. To help answer this question, a preliminary study has been conducted of the behavioral and biological effects of high-intensity 60-Hz electric fields on baboons [2]. This study was a thorough test of the apparatus and experimental protocols of a planned major study of electric-field effects. Baboons were chosen as the experimental animals primarily because they have a long history of being an excellent physiological and behavioral model for man.

Experimental data taken from animal experiments of this type must be carefully considered before extrapolating the results to humans. The most obvious biological difference is that animals and man are of different size and shape. This means that each will interact differently with the applied fields, and the differences will be manifested by the magnitude and distribution of the induced body currents.

As a first step in the extrapolation of 60-Hz electric-field effects on experimental animals to equivalent effects on man, it is necessary to have knowledge of the corresponding dosimetry for humans and animals as based upon induced current densities. For example, scaling relations for applied electric fields in experimental exposure facilities must be developed so